Published in final edited form as:
J Biol Chem. 2007 December 7; 282(49): 35502–35509. doi:10.1074/jbc.M705823200.

Keratocan and Lumican Regulate Neutrophil Infiltration and Corneal Clarity in Lipopolysaccharide-induced Keratitis by Direct Interaction with CXCL1*

Eric C. Carlson[‡,1], **Michelle Lin**[‡], **Chia-Yang Liu**[§], **Winston W-Y. Kao**[§], **Victor L. Perez**[¶], and **Eric Pearlman**[‡]

[‡]Department of Ophthalmology, Case Western Reserve University, Cleveland, Ohio 44106

[§]Department of Ophthalmology, University of Cincinnati, Cincinnati, Ohio 45267

[¶]Department of Ophthalmology, University of Miami, Miami, Florida 33136

Abstract

Keratocan and lumican are keratan-sulfate proteoglycans (KSPG), which have a critical role in maintaining corneal clarity. To determine whether these KSPGs have a role in corneal inflammation, we examined *Kera*$^{-/-}$ and *Lum*$^{-/-}$ mice in a model of lipopolysaccharide (LPS)-induced keratitis in which wild-type mice develop increased corneal thickness and haze due to neutrophil infiltration to the corneal stroma. Corneal thickness increases caused by LPS mice were significantly lower in *Kera*$^{-/-}$ and *Lum*$^{-/-}$ than wild-type mice. Further, LPS-injected *Lum*$^{-/-}$ mice had elevated corneal haze levels compared with that of *Kera*$^{-/-}$ and wild-type. At 24 h post-injection, total enhanced green fluorescent protein-positive bone marrow-derived inflammatory cells in chimeric mice was significantly lower in *Kera*$^{-/-}$ mice and *Lum*$^{-/-}$ mice compared with wild-type mice. Neutrophil infiltration was inhibited in *Kera*$^{-/-}$ and *Lum*$^{-/-}$ mice at 6 and 24 h post-stimulation, with *Lum*$^{-/-}$ corneas having the most profound defect in neutrophil migration. Reconstitution of keratocan and lumican expression in corneas of *Kera*$^{-/-}$ and *Lum*$^{-/-}$ mice using adeno-keratocan and adeno-lumican viral vectors, respectively, resulted in normal neutrophil infiltration in response to LPS. Immunoprecipitation/Western blot analysis showed that lumican and keratocan core proteins bind the CXC chemokine KC during a corneal inflammatory response, indicating that corneal KSPGs mediate neutrophil recruitment to the cornea by regulating chemokine gradient formation. Together, these data support a significant role for lumican and keratocan in a corneal inflammatory response with respect to edema, corneal clarity, and cellular infiltration.

Corneal transparency is dependent on a tightly regulated, dynamic series of events, and disruption of normal homeostatic regulatory processes can result in loss of corneal clarity, visual impairment, and in severe instances corneal opacification and blindness. One critical requirement for corneal clarity is maintenance of the highly organized matrix of collagen fibrils. This organization of collagen fibrils with respect to fibril diameter and interfibrillar

*This work was supported by National Institutes of Health Grants EY10320 and EY11373 (to E. P.), EY11845 (to W. W. K.), and K08 EY014912 (to V. L. P.), NEI, National Institutes of Health Grant RO1 12486 (to C. Y. L.), the Research to Prevent Blindness Foundation, and Ohio Lions Eye Research Foundation. The costs of publication of this article were defrayed in part by the payment of page charges. This article must therefore be hereby marked "*advertisement*" in accordance with 18 U.S.C. Section 1734 solely to indicate this fact.

[1]To whom correspondence should be addressed: Dept. of Ophthalmology and Visual Sciences, Case Western Reserve University, 10900 Euclid Ave., Cleveland, OH 44106-7286. Fax: 216-368-3713; Eric.Carlson@case.edu..

spacing is regulated largely by lumican and keratocan, which are part of the small leucine-rich keratan-sulfate proteoglycan (KSPG)[2] family (1–3). Keratocan expression is limited to the corneal stroma in adult mice, whereas lumican is also expressed in skin, sclera, and aorta (4, 5).

The role of KSPGs in maintaining corneal clarity has been shown in keratocan-null mice (*Kera*$^{-/-}$), which have an overall thinner corneal stroma and a narrower cornea-iris angle as compared with wild-type littermates (3). In contrast, corneas of lumican-null mice (*Lum*$^{-/-}$) are also thinner but also have corneal opacity (6). Corneal inflammation caused by active microbial infection or by microbial products leads to decreased visual acuity, primarily as a result of inflammatory cell infiltration. Neutrophils are the predominant infiltrating cells, and their degranulation and release of cytotoxic mediators can disrupt normal corneal function (7–9). Several reports show that neutrophil recruitment is mediated by CXC chemokines produced by resident corneal cells, which have an important role in neutrophil recruitment to the corneal stroma (10–12); however very little is known about the role of extracellular matrix proteins, including KSPGs in neutrophil infiltration.

In the current study, we used gene knock-out mice to examine the role of lumican and keratocan in regulating neutrophil recruitment and loss of corneal clarity. Our results demonstrate that KSPGs have a critical role in the corneal inflammatory response. Furthermore, we identify a novel role for corneal proteoglycans during an inflammatory response by showing that keratocan and lumican bind CXCL1/KC.

EXPERIMENTAL PROCEDURES

Animals

C57BL/6-TgN(ACTbEGFP)1Osb (The Jackson Laboratory), B6/129, *Kera*$^{-/-}$, and *Lum*$^{-/-}$ mice (26) 8–12 weeks of age were utilized in this study after pre-operative examination for exclusion criteria such as ocular disease, wound, or infection. Animal care and use conformed to the Association for Research in Vision and Ophthalmology Resolution on the Use of Animals in Research. The Institutional Care and Use Committee of Case Western Reserve University approved all animal protocols. Mice were anesthetized by intraperitoneal injections of ketamine (2.0 mg) and xylazine (0.4 mg). One drop of Alcaine® 0.5% proparacaine hydrochloride ophthalmic solution (Alconlabs, Fort Worth, TX) was applied to each eye prior to surgery as a topical anesthetic.

Generation of EGFP Chimeric Mice

C57BL/6 recipient mice received a total of 1,200 rads (12 grays) whole body irradiation delivered in two doses of 600 rads (6 grays) 3 h apart as previously described (10, 13, 14) and were then injected intravenously (tail vein) with 5×10^6 bone marrow cells from the C57BL/6-TgN (ACTbEGFP) (Jackson Laboratory). Enhanced green fluorescent protein (EGFP) chimeric mice were used 2 weeks after the bone marrow transplant to allow for bone marrow reconstitution (15).

Induction of LPS Keratitis

Intrastromal injection of 1 μg (EGFP chimeric experiments) or 500 ng of ultrapure *Escherichia coli* LPS (Invivogen) in 2–3 μl of PBS (Sigma) or PBS only was performed in sedated animals as previously described (16, 17). Briefly, a small tunnel from the corneal

[2]The abbreviations used are: KSPG, keratan-sulfate proteoglycan; LPS, lipopolysaccharide; EGFP, enhanced green fluorescent protein; PBS, phosphate-buffered saline; IP, immunoprecipitation; hKera, human keratocan; hLum, human lumican; KC, keratinocyte-derived chemokine; ELR, glycineleucine-arginine motif.

epithelium to central stroma was created using a 33-gauge needle (Hamilton Co., Reno, NV). Another 33-gauge needle attached to a 10-μl Hamilton syringe was passed through the tunnel into the central cornea where the contents of the syringe were injected.

Adenoviral in Vivo Transfection

The mice were subjected to intrastromal injection of adenoviral vectors (Ad-Lum, Ad-Kera, and Ad-EGFP) as described previously (16) and observed during a recovery period until awakening in a heated chamber. Expression was confirmed by visualizing EGFP-positive cells 18 h following the introduction of the adenoviral constructs to the corneal stroma. Fluorescent stereomicrograph EGFP intensity was quantitated using Image Pro Plus (Media Cybernetics Inc., Carlsbad, CA).

Construction of Recombinant Adenoviruses

The human keratocan (*hKera*) and lumican (*hLum*) full-length coding regions were generated by reverse transcription-polymerase chain reaction using total RNA isolated from human cornea (Cincinnati Eye Bank). The PCR primers for *hKera* were: hKera > 5′, gatcgcggccgctata atggcaggcacaatctgtttc, and hKera > 3′, gatcgcggccgcgtttaaataatgacagcctgcagaa, and for *hLum* were Lum > 5′, gatcgcggccgcaaaatgagtctaagtgcatttactc, and Lum > 3′, gatcgcggccgcgat attaattaagagtgacttcgtt. The resulting PCR products were then subcloned into the NotI site of pcDNA3.1(+) (Invitrogen, Inc.). Both *hKera* and *hLum* cDNA in the constructed plasmid were confirmed by DNA sequencing. The *hKera* and *hLum* fragments were then excised from pcDNA3.1-*hKera* and pcDNA3.1-*hLum* plasmid, respectively, with NotI and inserted into the pAdTrack-CMV pAdTrack-CMV to yield an adenoviral shuttle plasmids. Recombinant adenoviral plasmids were generated by homologous recombination in *E. coli*, as described previously (18). Purified viruses were aliquoted in 50% glycerol and stored at −20 °C. The viral titer (plaque-forming unit per ml) for adenovirus preparation was determined in 293 cells using 96-well plates and series-diluted virus for transfection. After 7 days, green fluorescent protein expression was examined under an inverted fluorescence microscope to calibrate the viral titer.

In Vivo Imaging

Imaging of EGFP-positive inflammatory cell migration into the cornea was performed using a Leica MZFLIII high resolution stereo fluorescence microscope with a vertical fluorescence illuminator (Leica Microsystems Inc., Bannockburn, IL). Sedated EGFP chimeric mice were immobilized using a custom-built three-point stereotactic mouse restrainer, and images were captured at different time points using a SpotCam RT KE digital camera (Sterling Heights, MI). Images were obtained at 32× magnification using a standardized exposure time. EGFP-positive cells were quantitated using Image Pro Plus (Media Cybernetics Inc., Carlsbad, CA).

Immunohistochemical Staining of Cornea Frozen Sections

Eyes were enucleated 24 h after intrastromal injection, snap frozen, and embedded in Tissue-Tek® OCT compound (Miles Scientific, Naperville, IL). 5-μm frozen sections of the central cornea were air dried for 30 min, fixed in 4% paraformaldehyde for 30 min at room temperature, and washed with PBS, and neutrophils and macrophages were stained with anti-NIMP-R14 (Serotec, Oxford, UK) and anti-F4/80 (Serotec), respectively. NIMP-R14 recognizes a currently undetermined structure on the neutrophil plasma membrane and has been successfully used to identify neutrophils in murine corneas (19).

Examination of Stromal Thickness and Haze

In vivo analysis of cellular infiltration was accomplished by *in vivo* confocal microscopy (Confoscan3; Nidek Technologies America, New Orleans, LA) as described (20). Briefly, mice were anesthetized and immobilized on a secure platform. A ×40 objective was maneuvered into place on the corneal surface by using transparent gel (Genteal; Novartis Ophthalmics, Duluth, GA) as a medium between the corneal surface and the objective, and the software (NAVIS; Lucent Technologies, Murray Hill, NJ) captured images every 1.3 μm and stored them as a stack for analysis of corneal thickness and haze.

Stromal thickness was defined as the area between basal epithelium and corneal endothelium, and stromal haze was defined as stromal thickness×combined light intensity of each image of the corneal stroma. To obtain this, the series of intensity values for each corneal stroma was used to generate and calculate the total area under the curve (Prism; Graph Pad Software, San Diego, CA). Base-line measurements were determined from PBS-injected mouse corneas.

Immunoprecipitation/Western Blot Analysis

Corneas were excised 24 h after intrastromal injection of 500 ng of LPS and homogenized using a TissueLyser in IP buffer (Protein G Immunoprecipitation kit; Sigma-Aldrich). Following homogenization, individual corneas were aliquoted and either 5 μg of rat anti-KC or rat IgG2a antibodies (R&D Systems Inc. Minneapolis, MN) were added to the aliquots, placed in the supplied tubes from the Sigma Protein G Immunoprecipitation kit, and incubated for 5 h at 4 °C. Following this incubation, Protein G was added and incubated overnight at 4 °C. The column was centrifuged (12,000 × *g*), washed two times with 0.1% SDS and 0.5 M NaCl in 1× IP buffer, and washed four more times with 1× IP buffer. The final wash was performed with 0.1× IP buffer. Samples were eluted with 2× Laemelli buffer and heated to 95 °C for 5 min. Samples were loaded equally for each cornea and run on a 12.5 or 10% Fluorescent Sprint Gel, transferred to polyvinylidene difluoride membrane, and blocked with 5% cold water fish gelatin (AMRESCO, Solon, OH). Western blots for lumican and keratocan were performed as previously described (21).

Statistical Analysis

A one-way analysis of variance with a Tukey post hoc test was performed at a 95% confidence interval for Figs. 1, 2, and 3. Values listed are *p* values of the Tukey post hoc test when $p < 0.05$. A Student's two-tailed *t* test was performed at a 95% confidence interval for the data presented in Fig. 5. *p* values are listed. Statistical analyses were performed using GraphPad Prism software (GraphPad Software Inc.).

RESULTS

KSPG-null Corneal Thickness and Stromal Haze during an LPS-induced Inflammatory Response

One outcome of corneal inflammation is the development of corneal opacity and edema, which lead to transient or permanent vision loss. Naïve $Lum^{-/-}$ mice have significantly greater corneal opacity and overall thinner corneas when compared with naïve wild-type corneas whereas $Kera^{-/-}$ mice exhibit a thin but transparent corneal phenotype (3).

To determine the role of lumican and keratocan in LPS keratitis, we measured corneal thickness and haze in KSPG-null mouse corneas ($n = 4$). PBS or LPS was injected into the corneal stroma of $Lum^{-/-}$, $Kera^{-/-}$, and wild-type littermate controls, and *in vivo* confocal microscopy (Confoscan^{TM}) was used to measure stromal thickness 24 h following intrastromal injection. As shown in Fig. 1*A*, PBS-injected corneas showed a significant

difference in thickness between the groups, with $Lum^{-/-}$ < $Kera^{-/-}$ < control mice and following LPS injection (Fig. 1*B*), $Kera^{-/-}$ and $Lum^{-/-}$ corneal thickness remained less than wild-type corneas.

For corneal haze, PBS-injected $Lum^{-/-}$ mouse corneas were significantly higher than $Kera^{-/-}$ and wild-type corneas (Fig. 1*C*). However, LPS-injected $Lum^{-/-}$ corneas had elevated haze compared with wild-type and $Kera^{-/-}$ (Fig. 1*D*), suggesting that the absence of lumican and the decreased expression of keratocan in the corneal stroma of $Lum^{-/-}$ mice results in a collagen matrix more susceptible to edema. Increased edema in the corneal stroma results in a more disorganized collagen matrix leading to increased corneal haze. The lack of uniformity in collagen fibril diameter inherent to $Lum^{-/-}$ mice and increased interfibrillar spacing also contributes to elevated haze in these mice.

Together, these data show that keratocan is important in the regulation of cornea stromal thickness but has little impact on corneal transparency. However, our findings demonstrate that lumican is a critical component in development of LPS-induced increased stromal thickness and loss of corneal transparency.

Bone Marrow-derived Inflammatory Cell Infiltration Is Inhibited in $Kera^{-/-}$ and $Lum^{-/-}$ Corneas during LPS-induced Keratitis

To examine the role of keratocan and lumican on cellular infiltration, $Kera^{-/-}$ and $Lum^{-/-}$ mice were lethally irradiated (12 grays) and reconstituted with EGFP-positive bone marrow cells extracted from the C57BL/6-TgN (ACTbEGFP) mouse, as previously reported (10). Following bone marrow reconstitution (2 weeks), $Kera^{-/-}$ and $Lum^{-/-}$ × EGFP chimeric mice were injected intrastromally with 2 μg of LPS. *In vivo* fluorescent stereomicroscope images were taken at 24 h (Fig. 2*A*) post-LPS injection to determine the kinetics of bone marrow-derived inflammatory cell infiltration into these corneas. The representative images (n = 3) show EGFP-positive bone marrow-derived inflammatory cells present in wild-type, $Kera^{-/-}$, *and* $Lum^{-/-}$ chimeric mouse corneas 24 h after injection of LPS into the corneal stroma. The total number of EGFP+ bone marrow-derived cells present in the corneas (paracentral to central) 24 h following intrastromal injection were measured using ImagePro + software. Fig. 2*B* shows that, as in our previous study, wild-type chimeric mice injected with 2 μg of LPS developed a pronounced cellular infiltrate (2). In the current study, these mice had EGFP+ cells (1,058 ± 38) in the cornea. In contrast, EGFP+ cells in $Kera^{-/-}$ (616 ± 139) and $Lum^{-/-}$ (327 ± 55) were significantly reduced. There was no significant difference between $Kera^{-/-}$ and $Lum^{-/-}$ corneas. Taken together, these data indicate that bone marrow cell infiltration to the corneal stroma is dependent on both lumican and keratocan.

Keratocan and Lumican Are Essential for Neutrophil Infiltration to the Corneal Stroma

Our previous studies using this model showed that the neutrophil infiltrate peaked at 24 h after LPS injection (10). To determine the role of these KSPGs on neutrophil infiltration, LPS keratitis was induced by injecting LPS into the corneal stroma of wild-type, $Lum^{-/-}$, and $Kera^{-/-}$ mice (n = 5). After 6 and 24 h, eyes were enucleated, and 5-μm sections were immunostained using the neutrophil marker NIMP-R14. As shown in Fig. 3, $Kera^{-/-}$ and $Lum^{-/-}$ corneas had significantly fewer neutrophils in the corneal stroma at 6 and 24 h. Furthermore, $Lum^{-/-}$ corneas had significantly fewer neutrophils than the $Kera^{-/-}$ corneas. These data show that keratocan and lumican regulate neutrophil infiltration through the cornea stroma.

ELR+ CXC Chemokine Production Is Not Reduced in Kera$^{-/-}$ and Lum$^{-/-}$ Corneas

One possible mechanism underlying the impaired ability of neutrophils to infiltrate *Kera*$^{-/-}$ and *Lum*$^{-/-}$ corneas is decreased ELR+ CXC chemokine expression. ELR+ CXC chemokines mediate neutrophil recruitment to the cornea during an LPS-induced inflammatory response (12, 21). *Kera*$^{-/-}$, *Lum*$^{-/-}$, and wild-type mice ($n = 5$) were injected with LPS as before, and after 6 h corneas were dissected and homogenized, and enzyme-linked immunosorbent assay was used to measure KC/CXCL1 and MIP-2/CXCL2 levels.

As shown in Fig. 4, KC and MIP-2 were produced by all three strains, and there was no significant difference among any of the groups. This finding indicates that impaired neutrophil infiltration is not due to differences in ELR+ CXC chemokine production.

Rescue of KSPG-null Phenotype Using Adenoviral Constructs

We previously demonstrated that adenoviral vectors are expressed in the corneal stroma for up to 21 days after injection (16). To determine whether adenovirus expressing keratocan or lumican can rescue the phenotype of these mice after LPS injection, adenovirus constitutively expressing *hLumican*, *hKeratocan*, and EGFP under the cytomegalovirus promoter was intrastromally injected into the corneal stroma of KSPG-null mice 18 h prior to LPS (500 ng) intrastromal injection. Adenoviral-delivered transgene expression in wild-type mice was confirmed by EGFP standardized expression between the ad-hLum and ad-hKera constructs as shown in Fig. 5*A*. Transgene expression was confirmed by visualizing EGFP expression under a fluorescent stereomicroscope (Fig. 5*B*). The kinetics of ad-EGFP empty vector expression was described previously (16). 6 and 24 h following LPS injection, 5-μm corneal sections were immunostained for NIMP-R14, as before. Fig. 5*C* shows that at 6 h following LPS injection, adeno-hKera-injected corneas ($n = 3$) had a 3.6-fold increase ($p = 0.031$) of neutrophils in the cornea as compared with control adeno-EGFP corneas in *Kera*$^{-/-}$ mice (Fig. 5*A*). Similarly, *Lum*$^{-/-}$ corneas ($n = 3$) injected with adeno-hLum constructs had a 3.2-fold increase ($p = 0.047$) of neutrophils as compared with the adeno-EGFP-injected corneas (Fig. 5*D*). At 24 h following LPS injection, *Kera*$^{-/-}$ corneas ($n = 5$) receiving adeno-hkera had a significantly greater number of neutrophils ($p = 0.028$) compared with control adeno-EGFP constructs (Fig. 5*E*). *Lum*$^{-/-}$ corneas ($n = 5$) injected with adeno-hLum prior to LPS stimulation had a significantly greater number of neutrophils present in the cornea ($p < 0.0001$) after 24 h (Fig. 5*F*). Therefore, the ability of neutrophils to migrate into the *Kera*$^{-/-}$ (Fig. 5, *C* and *E*) and *Lum*$^{-/-}$ (Fig. 5, *D* and *F*) mice was restored in mice receiving the corresponding adenoviral construct as compared with the empty vector control groups (Ad-EGFP). These differences were due to LPS-induced inflammation rather than intrinsic effects (or contaminants) relating to the adenoviral injections, as neutrophils were not recruited to naïve corneas or corneas injected with PBS (not shown).

KC Forms a Complex with Keratocan and Lumican Core Protein during an Inflammatory Response

Previous studies showed that CXCL1/KC mediates neutrophil recruitment in LPS-injected corneas (12), and others showed that CXCL1/KC binds to the proteoglycan syndecan 1 (22). To ascertain whether a similar mechanism is involved in *Kera*$^{-/-}$ and *Lum*$^{-/-}$ mice, we determined whether KC is able to bind keratocan and/or lumican during LPS keratitis. To examine this possibility, corneas were injected with 500 ng of LPS, and corneal extracts were prepared by homogenizing in 1× IP buffer and incubated with anti-KC. KC was immunoprecipitated from the corneal extracts ($n = 4$) using rat anti-KC. Normal rat IgG2a served as a control and was incubated with an equal aliquot of the corneal extracts. Following high stringency washing (5 M NaCl and 0.1% SDS), the samples were eluted, run on a 12.5% Fluorescent Sprint gel (AMRESCO), and Western blots for keratocan and lumican were performed.

Fig. 6 shows the presence of keratocan core protein (Fig. 6*A*, *top panel*) in the samples immunoprecipitated with anti-KC, whereas no signal was detected in the Rat IgG2a control samples. Similarly, the presence of lumican core protein is detected in the samples immunoprecipitated with anti-KC (*bottom panel*).

To determine whether lumican and keratocan core protein or their keratan-sulfate side chains were responsible for binding KC, corneas were injected with LPS and 24 h later corneal extracts were prepared and equally aliquoted. One aliquot was digested with keratanase to remove all keratan sulfation prior to washing and eluting the immunoprecipitates, while the other aliquot remained undigested. Samples were then run on a 10% Fluorescent Sprint gel (AMRESCO), and Western blot for keratocan (Fig. 6*B*, *top panel*) or lumican (*bottom panel*) was performed. This demonstrates identical size proteins were immunoprecipitated with anti-KC in both the keratanase-digested and undigested samples. No higher molecular weight bands indicative of glycosylation were detected in the untreated samples. This finding indicates that the binding of KC is to the core protein and not to the keratin-sulfate chains. These results demonstrate that KC specifically binds keratocan and lumican core protein during an LPS-induced inflammatory response in the cornea and demonstrate an important role for these KSPGs in neutrophil infiltration to the corneal stroma.

DISCUSSION

The results presented in this study demonstrate a significant role for corneal proteoglycans in the process of neutrophil infiltration during an innate immune response. The use of *Lum*$^{-/-}$ and *Kera*$^{-/-}$ mice demonstrates the role of these KSPGs in regulating neutrophils to infiltrate the corneal stroma, especially in *Lum*$^{-/-}$ corneas. Bone marrow stromal cells express lumican (23), suggesting that these cells could contribute to the observed phenotype. However, *Lum*$^{-/-}$ and *Kera*$^{-/-}$ mice reconstituted with wild-type bone marrow cells had impaired responses to LPS compared with wild-type recipients, indicating that the inhibition of neutrophil infiltration is the direct result of alteration of the extracellular matrix in the cornea. The restoration of lumican and keratocan expression in corneas using *in vivo* adenoviral infection conferred a wild-type phenotype to *Lum*$^{-/-}$ and *Kera*$^{-/-}$ mice, thereby supporting the bone marrow chimera results in showing that KSPG expression in the keratocytes, rather than bone marrow-derived cells, is the essential mediator of inflammation. Also, as is evident in other data presented in this study, the impact of lumican was notably greater than its KSPG family member keratocan.

Taking these findings together, it is clear that the keratansulfate proteoglycans play a critical role in the inflammatory response and that these KSPG regulate inflammation by the specific binding of KC to keratocan and lumican. This direct interaction implicates both a novel and an important role for keratan-sulfate proteoglycans in the inflammatory response. KC also binds syndecan-1, a cell-bound heparan-sulfate proteoglycan, in a model of acute lung injury. The underlying mechanism was hypothesized to be that the interaction is necessary for formation of a chemokine gradient responsible for bringing neutrophils from the interstitium to the alveolar space. When bound, KC is unable to diffuse through the matrix to form a chemotactic gradient for neutrophil influx. However, matrilysin cleaves syndecan from the cell surface, which releases the syndecan-1/KC complex, allowing for the formation of a chemokine gradient. This gradient then allows neutrophils to be recruited to the site of inflammation (22). We propose a similar mechanism in the cornea to bring neutrophils from the limbal vessels into the corneal stroma.

Lumican is reported to regulate gene expression (21), cell proliferation (24), cell migration, cell adhesion (25), and wound healing (26). Following a corneal epithelial debridement

injury, lumican-null mice have delayed epithelial wound healing that is attributed to impaired cell migration and proliferation (26). Moreover, lumican is capable of regulating keratocan gene expression through transcriptional regulation in the corneal stroma. Keratocan expression is significantly decreased in lumican-null mice, whereas lumican expression is unchanged in keratocan-null mice (27). *Kera*$^{-/-}$ mice express lumican at normal levels in the cornea, but *Lum*$^{-/-}$ mice have a significant reduction in keratocan expression. Furthermore, reporter gene expression driven by the keratocan promoter when co-expressed with lumican resulted in a 2-fold increase in activity. This not only demonstrates the ability of lumican to regulate gene expression at the transcriptional level but also provides insight as to why *Lum*$^{-/-}$ mice have a more pronounced phenotype than Kera$^{-/-}$ mice with respect to decreased corneal clarity, thinner corneal stroma, and a significantly greater impairment of neutrophil infiltration.

The impaired recruitment of neutrophils in *Lum*$^{-/-}$ corneas during an inflammatory response due to epithelial injury and topical exposure to LPS was previously reported as being dependent upon impaired expression of the pro-inflammatory cytokines tumor necrosis factor α, interleukin 1β, and interleukin 6 (28). This same group recently reported that *Lum*$^{-/-}$ are hyporesponsive to LPS-induced septic shock and the systemic administration of LPS also resulted in decreased serum levels of the same pro-inflammatory cytokines (29). We also found a similar finding in *Lum*$^{-/-}$ mice with respect to decreased neutrophil infiltration but report a different mechanism for Lum$^{-/-}$ and *Kera*$^{-/-}$ corneas.

CXC chemokines also mediate neutrophil recruitment to the cornea during an LPS-induced inflammatory response, specifically the ELR+ CXC chemokines (LIX, KC, MIP-2) (12). CXC chemokines are expressed by resident macrophages and corneal fibroblasts in response to LPS stimulation (12). Here, we report no difference in ELR+ CXC chemokine expression in *Lum*$^{-/-}$ mice, suggesting there is no reduction in the expression of chemokines responsible for corneal neutrophil infiltrates. We have demonstrated that levels of these chemokines in the *Lum*$^{-/-}$ and *Kera*$^{-/-}$ corneas are not significantly different from wild-type corneas, implying that *Lum*$^{-/-}$ and *Kera*$^{-/-}$ mice effectively produce the factors necessary to elicit an innate immune response to recruit neutrophils to the cornea. Moreover, neutrophils extravasate from the limbal vessels and migrate into the cornea in the proteoglycan-null corneas, albeit at a reduced level. Because the levels of the chemokines responsible for corneal infiltration of neutrophils are not suppressed, it is possible these chemokines are not active. The ability of proteoglycans to bind chemokines rendering the chemokine inactive has been documented in instances of hepatitis and acute lung inflammation. It has been suggested that in these models the proteoglycan binds the chemokine, rendering it inactive until the proteoglycan is cleaved, thereby releasing the complex. The release of this complex allows the chemokine to become active and establish the chemokine gradient necessary for recruitment of neutrophils to the site of inflammation (22, 30). In the current study, we found that KC binds lumican and keratocan, supporting the notion of a similar pathway in the cornea. This interaction suggests a potential function for keratocan and lumican in the cornea, i.e., to sequester and release chemokines in the extracellular matrix necessary for neutrophil infiltration.

The data presented here, taken together with previous reports, demonstrate that keratan-sulfate proteoglycans in the cornea have the potential to create a chemokine gradient necessary for neutrophil influx during a Gram-negative bacterial infection. *Lum*$^{-/-}$ and *Kera*$^{-/-}$ mice have an impaired ability to recruit neutrophils to the cornea in response to the bacterial endotoxin LPS. Identification of the factors responsible for the mobilization of this CXC chemokine/proteoglycan complex to form a gradient are currently underway to identify the mechanism whereby proteoglycans regulate the infiltration of neutrophils into the corneal stroma.

Acknowledgments

We thank Eugenia Diaconu, Sixto Leal (Case Western Reserve University), and Lung-Kun Yeh (Chang-Gung Memorial Hospital, Linko, Taiwan) for their technical support.

REFERENCES

1. Carlson EC, Mamiya K, Liu CY, Gendron RL, Birk DE, Funder-burgh JL, Kao WW. Biochem. J. 2003; 369(Pt. 3):461–468. [PubMed: 12381269]
2. Chakravarti S, Petroll WM, Hassell JR, Jester JV, Lass JH, Paul J, Birk DE. Investig. Ophthalmol. Vis. Sci. 2000; 41:3365–3373. [PubMed: 11006226]
3. Liu CY, Birk DE, Hassell JR, Kane B, Kao WW. J. Biol. Chem. 2003; 278:21672–21677. [PubMed: 12665512]
4. Ying S, Shiraishi A, Kao CW, Converse RL, Funderburgh JL, Swiergiel J, Roth MR, Conrad GW, Kao WW. J. Biol. Chem. 1997; 272:30306–30313. [PubMed: 9374517]
5. Liu C, Arar H, Kao C, Kao WW. Gene. 2000; 250:85–96. [PubMed: 10854782]
6. Chakravarti S, Magnuson T, Lass JH, Jepsen KJ, LaMantia C, Carroll H. J. Cell Biol. 1998; 141:1277–1286. [PubMed: 9606218]
7. Oshima T, Sonoda KH, Tsutsumi-Miyahara C, Qiao H, Hisatomi T, Nakao S, Hamano S, Egashira K, Charo IF, Ishibashi T. Br. J. Ophthalmol. 2006; 90:218–222. [PubMed: 16424537]
8. Pearlman E, Hall LR. Parasite Immunol. 2000; 22:625–631. [PubMed: 11123754]
9. Szliter EA, Barrett RP, Gabriel MM, Zhang Y, Hazlett LD. Eye Contact Lens. 2006; 32:12–18. [PubMed: 16415687]
10. Carlson EC, Drazba J, Yang X, Perez VL. Investig. Ophthalmol. Vis. Sci. 2006; 47:241–248. [PubMed: 16384969]
11. Khan S, Cole N, Hume EB, Garthwaite L, Conibear TC, Miles DH, Aliwaga Y, Krockenberger MB, Willcox MD. J. Leukocyte Biol. 2007; 81:315–318. [PubMed: 17028201]
12. Lin M, Carlson E, Diaconu E, Pearlman E. J. Leukocyte Biol. 2006; 81:786. [PubMed: 17110418]
13. Kozu T, Sueoka E, Okabe S, Sueoka N, Komori A, Fujiki H. Biochimie (Paris). 1996; 78:1067–1073.
14. Van Parijs L, Refaeli Y, Lord JD, Nelson BH, Abbas AK, Baltimore D. Immunity. 1999; 11:281–288. [PubMed: 10514006]
15. Auletta JJ, Devecchio JL, Ferrara JL, Heinzel FP. Biol. Blood Marrow Transplant. 2004; 10:834–847. [PubMed: 15570252]
16. Carlson EC, Liu CY, Yang X, Gregory M, Ksander B, Drazba J, Perez VL. Investig. Ophthalmol. Vis. Sci. 2004; 45:2194–2200. [PubMed: 15223795]
17. Stechschulte SU, Joussen AM, von Recum HA, Poulaki V, Moromizato Y, Yuan J, D'Amato RJ, Kuo C, Adamis AP. Investig. Ophthalmol. Vis. Sci. 2001; 42:1975–1979. [PubMed: 11481260]
18. Chen J, Huber BT, Grand RJ, Li W. J. Immunol. 2001; 167:1297–1305. [PubMed: 11466346]
19. Khatri S, Lass JH, Heinzel FP, Petroll WM, Gomez J, Diaconu E, Kalsow CM, Pearlman E. Investig. Ophthalmol. Vis. Sci. 2002; 43:2278–2284. [PubMed: 12091428]
20. Johnson AC, Heinzel FP, Diaconu E, Sun Y, Hise AG, Golenbock D, Lass JH, Pearlman E. Investig. Ophthalmol. Vis. Sci. 2005; 46:589–595. [PubMed: 15671286]
21. Carlson EC, Liu CY, Chikama T, Hayashi Y, Kao CW, Birk DE, Funderburgh JL, Jester JV, Kao WW. J. Biol. Chem. 2005; 280:25541–25547. [PubMed: 15849191]
22. Li Q, Park PW, Wilson CL, Parks WC. Cell. 2002; 111:635–646. [PubMed: 12464176]
23. Liu Y, Cooper PR, Barralet JE, Shelton RM. Biomaterials. 2007; 28:1393–1403. [PubMed: 17166582]
24. Ping Lu Y, Ishiwata T, Asano G. J. Pathol. 2002; 196:324–330. [PubMed: 11857496]
25. Funderburgh JL, Mitschler RR, Funderburgh ML, Roth MR, Chapes SK, Conrad GW. Investig. Ophthalmol. Vis. Sci. 1997; 38:1159–1167. [PubMed: 9152235]
26. Saika S, Shiraishi A, Liu CY, Funderburgh JL, Kao CW, Converse RL, Kao WW. J. Biol. Chem. 2000; 275:2607–2612. [PubMed: 10644720]

27. Carlson EC, Wang IJ, Liu CY, Brannan P, Kao CW, Kao WW. Mol. Vis. 2003; 9:615–623. [PubMed: 14654769]

28. Vij N, Roberts L, Joyce S, Chakravarti S. Investig. Ophthalmol. Vis. Sci. 2005; 46:88–95. [PubMed: 15623759]

29. Wu F, Vij N, Roberts L, Lopez-Briones S, Joyce S, Chakravarti S. J. Biol. Chem. 2007; 282:26409–26417. [PubMed: 17616530]

30. Gueders MM, Balbin M, Rocks N, Foidart JM, Gosset P, Louis R, Shapiro S, Lopez-Otin C, Noel A, Cataldo DD. J. Immunol. 2005; 175:2589–2597. [PubMed: 16081833]

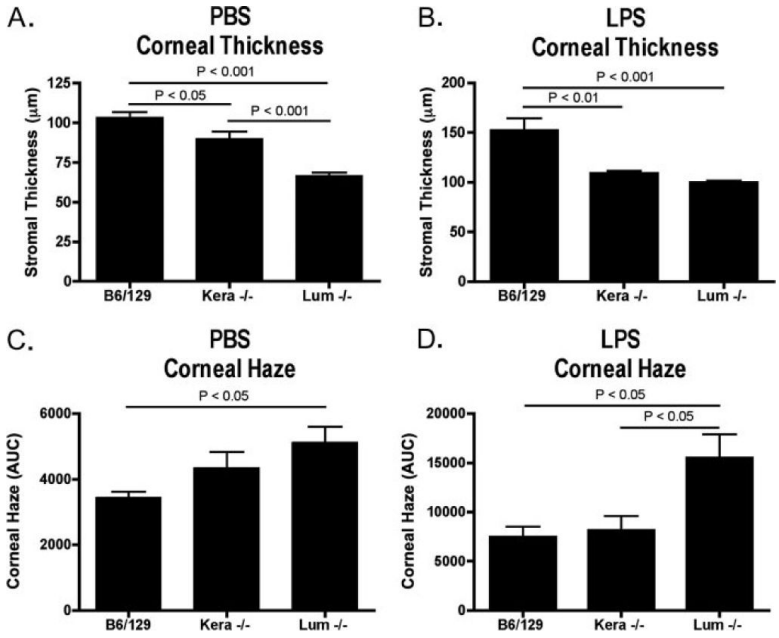

FIGURE 1. ***In vivo*** **confocal microscopy analysis of stromal thickness (*A*, *B*) and haze (*C*, *D*) in wild-type, *Kera*$^{-/-}$, and *Lum*$^{-/-}$ mice 24 h following a PBS or LPS (500 ng) intrastromal injection**

KSPG-null corneas injected with PBS exhibited an overall thinner corneal stroma compared with wild-type controls (*A*). This difference in stromal thickness increased further following an LPS-induced inflammatory response (*B*), demonstrating a resistance to increases in stromal thickness. Corneal haze was not significantly different between *Kera*$^{-/-}$ and wild-type controls, whereas *Lum*$^{-/-}$ mice exhibited significantly greater corneal haze following PBS injection (*C*). Corneal haze in LPS-injected *Kera*$^{-/-}$ mice did not differ from wild-type mice; however, *Lum*$^{-/-}$ mice further increased an already apparent difference in opacity (*D*). Note the difference in *y*-axis scales. *Error bars*, standard error of the mean.

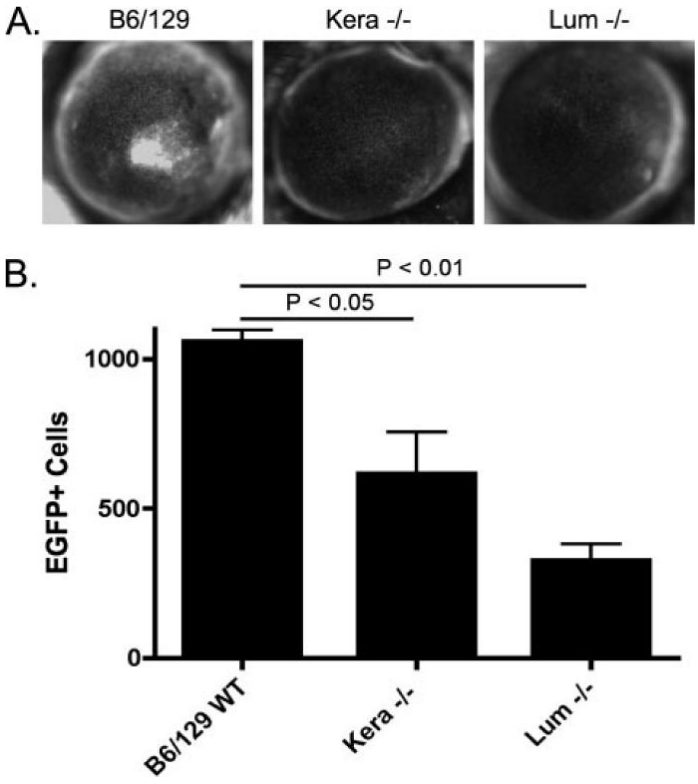

FIGURE 2. Kinetics of bone marrow-derived inflammatory cell infiltration into EGFP chimeric *Lum*$^{-/-}$ and *Kera*$^{-/-}$ mice inflammation

A, *in vivo* fluorescent stereomicrographs of B6/129 wild-type (B6/129), *Kera*$^{-/-}$, and *Lum*$^{-/-}$ × EGFP chimeric mouse corneas 24 h after intrastromal injection of LPS (1 μg). *B*, quantitation of EGFP-positive cells in chimeric mouse whole flat-mount corneas. *Error bars*, standard error of the mean.

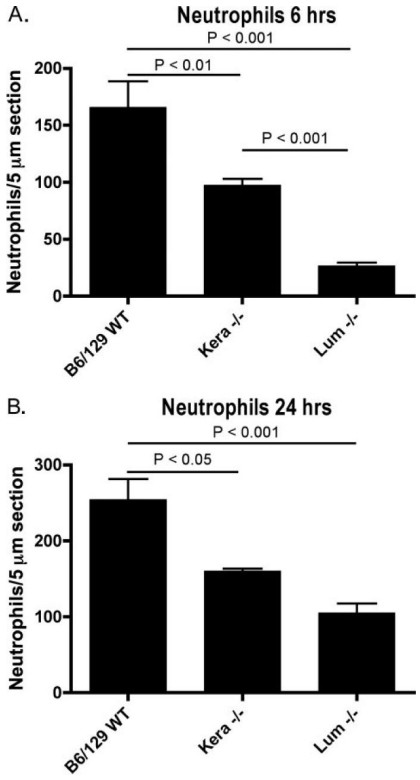

FIGURE 3. Impaired infiltration of neutrophils into Lumican and *Kera*$^{-/-}$ mice corneas 6 and 24 h following LPS-induced inflammation

The total number of neutrophils infiltrating wild-type, *Kera*$^{-/-}$, and *Lum*$^{-/-}$ corneas 6 (*A*) and 24 h (*B*) following intrastromal injection of 500 ng of LPS was quantitated as the number of NIMP-R14-positive cells/5-μm section. *Error bars*, standard error of the mean.

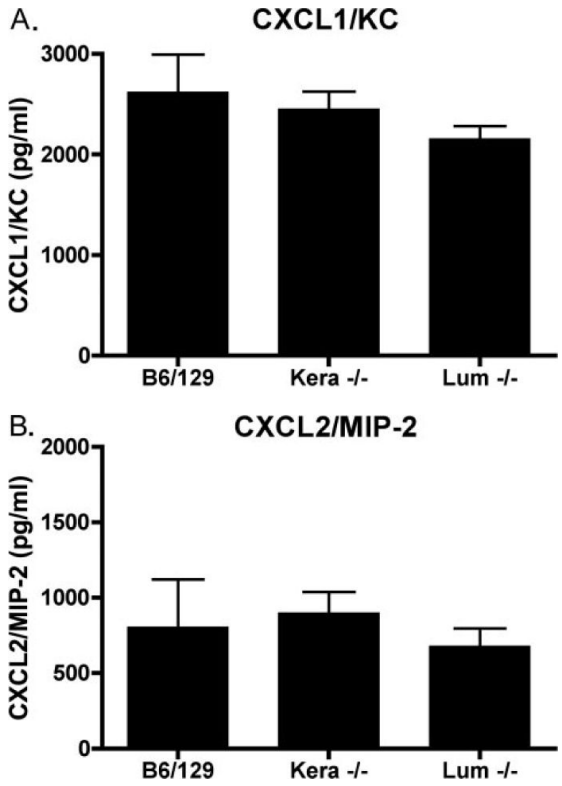

FIGURE 4. CXC chemokine expression in cornea of wild-type, *Kera*$^{-/-}$, and *Lum*$^{-/-}$ corneas

KC (*A*) and MIP-2 (*B*) expression measured by enzyme-linked immunosorbent assay in KSPG-null and wild-type corneas 6 h following intrastromal injection of LPS (500 ng). *Error bars*, standard error of the mean.

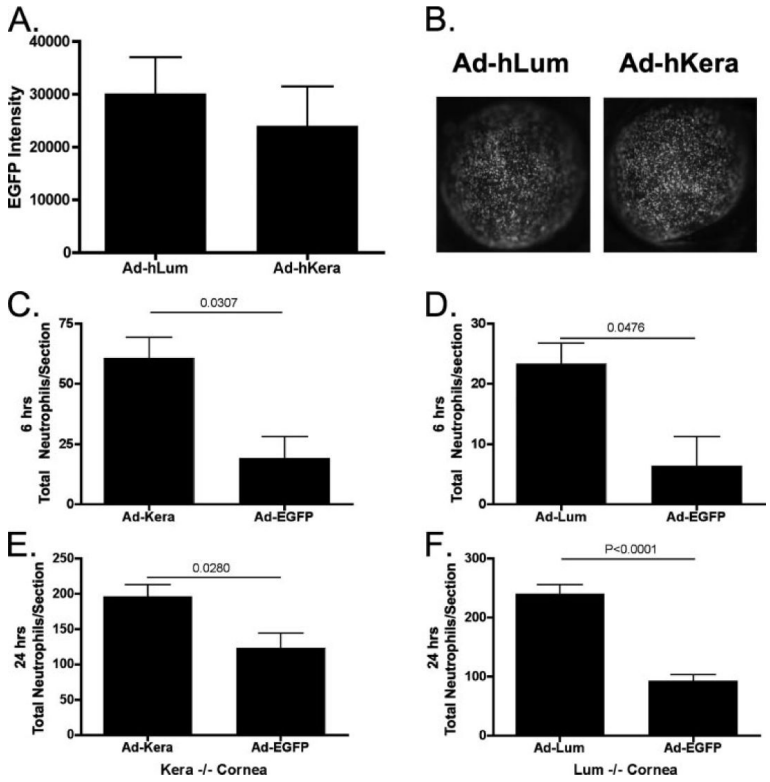

FIGURE 5. Reconstitution of *Kera*$^{-/-}$ and *Lum*$^{-/-}$ mice corneas *in vivo* was performed by intrastromal injection of adenoviral constructs expressing human Lumican (*Ad*-h*Lum*), keratocan (*Ad*-h*Kera*), or an EGFP control (*Ad-EGFP*)

EGFP expression was quantitated at 18 h post-injection (*A*) and corneas imaged using fluorescent stereomicroscopy (*B*) to confirm transgene expression. Following confirmation of transgene expression, 500 ng of LPS was injected intrastromally and neutrophils were quantitated using NIMP-R14 immunohistochemistry at 6 and 24 h for *Kera*$^{-/-}$ (*C*, *E*) and *Lum*$^{-/-}$ (*D*, *F*). *Error bars*, standard error of the mean.

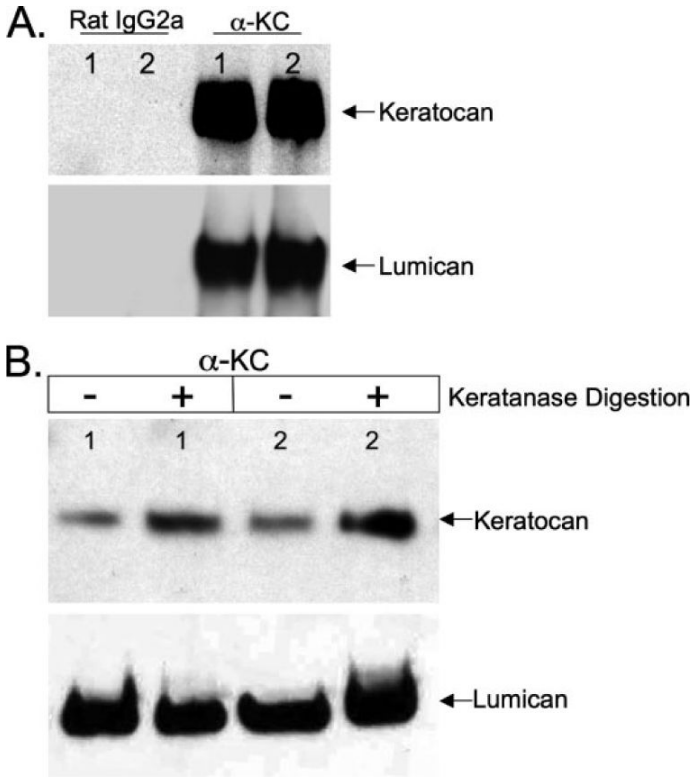

FIGURE 6.

Immunoprecipitation of the CXC chemokine KC from corneal extracts 24 h after LPS (1 μg) intrastromal injection followed by SDS-PAGE on a 12.5% gel and Western blots (*A*) for keratocan (*top*) and lumican (*bottom*). Rat IgG2a control immunoprecipitated samples show the absence of keratocan and lumican signals. Extracts from corneas excised 24 h following LPS injection were digested with keratanase prior to immunoprecipitation, and an equal aliquot was immunoprecipitated without keratanase digestion. Immunoprecipitates were then subjected to SDS-PAGE on a 10% gel and Western blot (*B*) for keratocan (*top*) and lumican (*bottom*). Exposure times for Western blots in *panel A* were greater in order to demonstrate the absence of signal in the IgG2a control lanes.